Correlated Charge Carrier-like Photoresponse of Polymer Nanowires

Atikur Rahman*,¶ and Milan K. Sanyal*

Surface Physics Division, Saha Institute of Nuclear Physics, 1/AF Bidhannagar, Kolkata 700 064, India. ¶Present address: (A.R.) Center for Functional Nanomaterials, Brookhaven National Laboratory, Upton, NY 11973, United States.

ABSTRACT Size confinement at nanometer length scales gives rise to many new and tunable properties of organic materials that are absent in their bulk state. Here we report, the appearance of large photoconduction property of a conducting polymer when it forms nanowires. The photoresponse and the external photoconductive gain were found to be >10^5 % and >200%, respectively, even at low bias (<1 V) voltage. These nanowires show a resistance switching transition at low temperature above a threshold bias, and below this transition, the resistance changes by more than 3 orders of magnitude under illumination of light. The photoresponse increases superlinearly and the resistance switching threshold voltage decreases with increasing illumination intensity. These properties are absent in the bulk polymer, and the observed photoresponse is not bolometric or excitonic in nature, nor it can be explained by free carrier generation or Schöttky barrier modulation, rather it is consistent with the photoexcitation of correlated charge carriers.

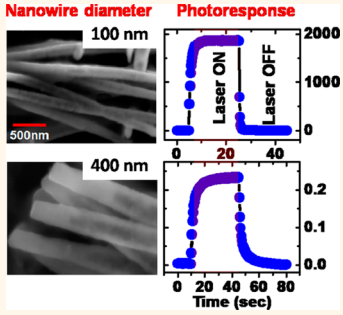

KEYWORDS: photoresponse · polymer nanowire · correlated electrons

Photoconducting materials are of intense importance for the development of photodetectors and photovoltaic cells, which have a wide range of applications such as environmental monitoring, optical communication, medical imaging, solar energy harvesting, space research, and defense applications.[1−13] Various mechanisms are responsible for photoconduction. Upon illumination with sufficient incident photon energy, electrons can be excited above the band gap, thereby creating a free electron and hole which contribute to conduction, provided their lifetime is longer than the transit time. On the other hand, if the photon energy is less than the band gap, an exciton (bound electron−hole pair) is created, which dissociates either thermally[14] or by a large electric field[15] to produce free carriers that increase the current. Photoconduction is also observed when incident light increases the temperature of the sample (bolometric response),[16] modulates the trap states at the surface or interface through photodesorption of adsorbed molecules, or modulates the Schöttky barrier formed at the interface.[17−19]

In pure polymer devices the main mechanism of electron transport is thermally (phonon) assisted hopping between localized (trap) states, so for incident light having energy below the band gap, photoconduction occurs mainly through the creation of excitons.[20−23] Owing to their poor mobility, single component pure polymer devices so far have shown only low photoresponse. Here, we demonstrate a new kind of photoconduction property of polypyrrole (PPy) when it forms nanowires. At low temperature these nanowires (having diameter up to 200 nm) show power-law behavior current−voltage ($I-V$) characteristics, resistance switching at relatively high bias, negative differential resistance (NDR), and noise enhancement in the switched state.[24,25] In the presence of 632.8 nm laser illumination at low temperature we observe large photoconductance both in the linear and nonlinear regions of the current−voltage characteristics, and the switching threshold voltage (V_{Th}) decreases with increasing illumination intensity. The photo current, $I_{ph} = (I_{light} - I_{dark})$, where $I_{light(dark)}$ is the current in the presence (absence) of light, increases superlinearly with increasing illumination intensity. The photoresponse (I_{ph}/I_{dark}) was found to be more than 10^5% and external photoconductive gain (G_{ext}), which is the ratio of photocurrent to incident photons, is greater than 2 even at low bias (<1 V). Bulk PPy does not show significant photoresponse upon 632.8 nm illumination (as it is unable

* Address correspondence to arahman@bnl.gov, milank.sanyal@saha.ac.in.

Received for review June 10, 2013 and accepted August 16, 2013.

Published online August 16, 2013
10.1021/nn402917h

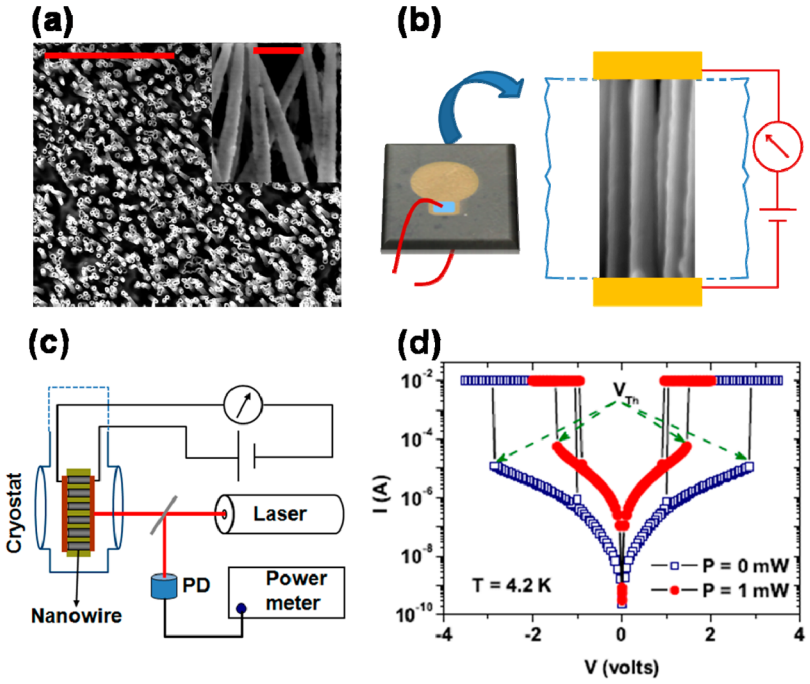

Figure 1. (a) Low magnification SEM image of the PPy nanowires synthesized using 200 nm pore diameter membrane (scale bar 10 μm). A higher magnification image of the nanowires is shown in the inset (scale bar 500 nm). (b) Picture of 10 nm thick 2 mm diameter gold contact (shown in false yellow color, where the laser is focused, and connecting wire is attached in the area shown in the blue rectangle) deposited PPy nanowire-embedded membrane. Schematic of cross-section of the device and measurement configuration are shown in the left panel. Gold contacts were deposited on both sides of the nanowire embedded membrane, thereby establishing a parallel connection with a large number (depends on the pore density of a particular membrane) of nearly monodisperse nanowires. The insulating polycarbonate matrix isolates the nanowires from each other. (c) Schematic view of the photoresponse measurement setup. (d) Current−voltage characteristics, measured at 4.2 K in the presence (solid circle) and absence (open square) of laser illumination. In the presence of illumination the current increases and the switching threshold voltage decreases. Also, the *I*−*V* characteristics remain symmetric.

to cause the $\pi-\pi^*$ transition which costs ~3.2 eV)[26] at our temperature (4.2−300 K) and bias (<4 V) ranges of interest. The observed large photoresponse cannot be explained by free carrier generation, exciton creation, bolometric effect, photoinduced desorption mechanism, or Schöttky barrier modulation. Rather, all the observations indicate the photoexcitation of correlated charge carriers present in these nanowires.

RESULTS AND DISCUSSION

Polypyrrole nanowires were synthesized using a porous template through chemical polymerization. Polycarbonate membranes of ~10 μm thickness and various pore diameters of 50, 100, 200, and 400 nm were used to synthesize the nanowires (see Methods and Supporting Information). Homogeneous formation of the nanowires over the entire membrane was confirmed by scanning electron microscopy (SEM) after the polycarbonate template was partially removed (see Figure 1a; for detailed characterization of theses nanowires, see Supporting Information, Figure S1a−d). Pellets of the bulk sample, made by the same concentration of chemicals and without taking the porous membrane, were used to compare the photoconduction property of the nanowires. Electrical characterization of these nanowires was done without removing the insulating polycarbonate membrane which isolates them from each other. A thin layer (10 nm) of gold was deposited on both sides of these nanowire-embedded membranes to make electrical contacts, as shown in Figure 1b (see Supporting Information for details). The low temperature photoconduction measurement schematic is shown in Figure 1c. Before the photoconduction measurement, we first studied the low temperature electronic transport properties of these samples. For nanowires up to 200 nm in diameter, we observe a sharp switching transition, NDR, and other features observed previously.[24,25] Nanowires synthesized using a 400 nm diameter membrane do not show any switching transition and behave like the bulk sample. Here we will present data of nanowires synthesized using a 200 nm pore diameter membrane; results of other diameter nanowires are discussed in the Supporting Information.

Figure 1d shows dc *I*−*V* characteristics of a typical nanowire synthesized using a 200 nm diameter membrane; the switching transition takes place at V_{Th} = 2.85 V at 4.2 K in the dark. Below the switching transition, the *I*−*V* characteristic is linear (Ohmic) at low bias, and at high bias power-law behavior is observed (see Supporting Information, Figure S2).[24,25] In the presence of laser illumination the current increases rapidly

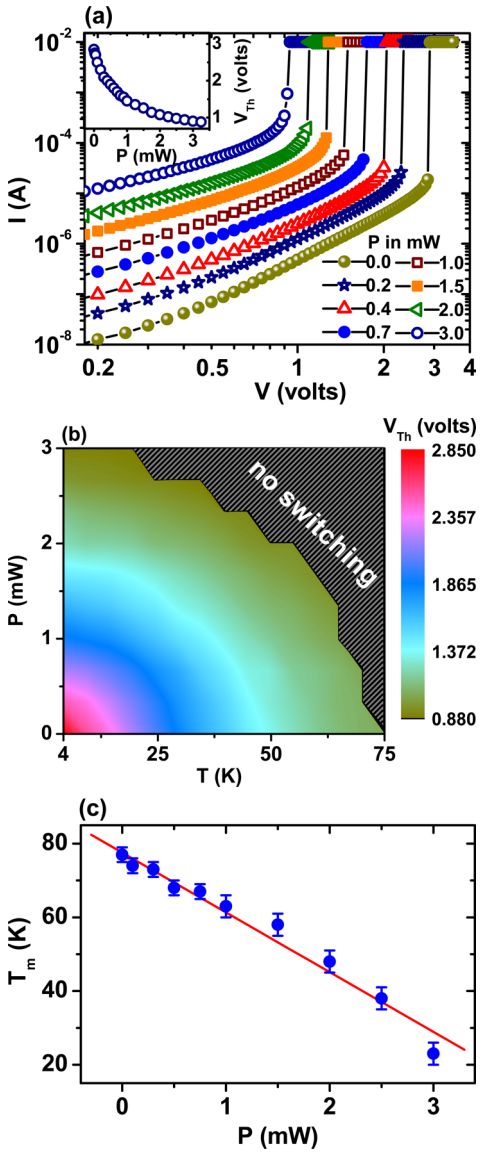

Figure 2. (a) Current−voltage characteristics measured at 4.2 K for various laser powers. Inset: variation of threshold voltage as a function of laser power. (b) Dependence of threshold voltage on temperature and laser power. It is clear that threshold voltage decreases with both increasing temperature and/or laser power. At low laser power, V_{Th} shows strong temperature dependence, and at higher power the dependence becomes weak. Above a certain temperature (T_m) switching behavior vanishes as shown by the shaded region. (c) T_m is plotted as a function of P (symbol) with a linear fit (line).

both in the linear and nonlinear regions of the $I-V$ characteristics, while the values of V_{Th} decrease. Representative data are shown in Figure 1d, where V_{Th} was reduced from 2.85 to 1.45 V in the presence of 1 mW laser illumination. The $I-V$ characteristics remain symmetric for both positive and negative bias voltage, and the hysteresis decreases under laser illumination (Figure 1d). This observation excludes the possibility of photocurrent generation as a result of Schöttky barrier modulation by illumination.[17−19] In our experiment the nanowires are illuminated from one end (see Figure 1c), so in a back-to-back Schöttky barrier configuration, the barrier of the illuminated side will only be modified (no detectable transmission of light is observed through the other end of the membrane containing nanowires (length $\approx 10\,\mu$m), even in the absence of gold coating), and the $I-V$ characteristics will be asymmetric resulting in different threshold voltages for positive and negative bias.

$I-V$ characteristics showing the switching transition at 4.2 K at various laser powers (P) are plotted in Figure 2a on a log−log scale, and the corresponding variation of V_{Th} as a function of P is shown in the inset. Below the switching transition, the photocurrent (I_{ph}) increases rapidly (superlinearly) with increasing P, both in the linear and nonlinear regions of the $I-V$ characteristics (see Supporting Information, Figure S3). In the absence of laser illumination, V_{Th} decreases with increasing temperature (see Supporting Information, Figure S4).[24,25] We have found that above a certain temperature (T_m) the switching behavior vanishes. With increasing P, the system becomes less sensitive to the temperature variation (see Supporting Information, Figure S5). Figure 2b shows the variation of V_{Th} with temperature for various laser powers. It is clear that in the absence of laser illumination, V_{Th} decreases rapidly with increasing temperature, but in the presence of illumination the threshold voltage shows relatively weak temperature dependence. With increasing P the switching behavior vanishes at relatively low temperature, that is, T_m decreases and the dependence is linear in P (Figure 2c). Above the switching transition the effect of light on the $I-V$ characteristics reduces precipitously (see Supporting Information, Figure S6).

The photoinduced relaxation characteristics, at various temperatures and laser intensities, have been studied by switching the laser illumination on and off and measuring the transient response. Figure 3a shows the photoresponse of these nanowires, with 0.8 V bias at 4.2 K, by switching a 4 mW laser illumination on and off. The response shows good repeatability over several on/off cycles. A similar response is observed in the linear region of the $I-V$ characteristics (see Supporting Information, Figure S7). When the laser is switched on or off, the photoresponse takes time to reach its equilibrium value. The transient photocurrent, $I_{ph}(t)$, shows an exponential time dependence, $I_{ph}(t) \alpha \exp(-t/\tau)$, where τ denotes a characteristic relaxation time. The value of τ ranges between 500 and 900 ms. Although the photoresponse decreases rapidly with increasing temperature (Figure 3b left panel), τ does not show significant temperature dependence for a fixed laser intensity. The photoresponse increases superlinearly with increasing P (Figure 3b right panel). At $P = 3.5$ mW and 0.85 V bias, the measured value of responsivity (defined as photocurrent flowing through a sample divided by incident optical power, I_{ph}/P) was found to

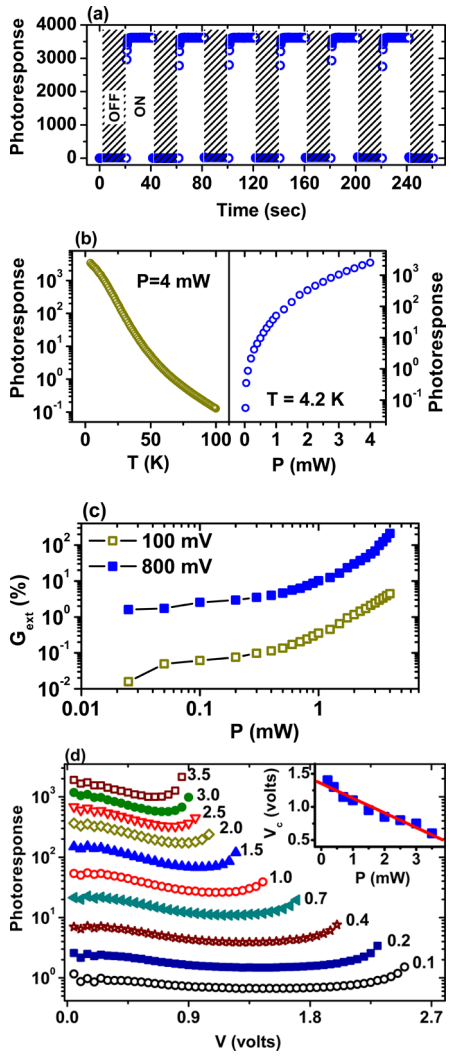

Figure 3. (a) Photoresponse measured at 0.8 V bias under periodic on and off (unshaded/shaded) 4 mW laser illumination of 632.8 nm wavelength. (b) Temperature dependence of the photoresponse in the presence of 4 mW illumination (left panel). The right panel shows the photoresponse (at 4.2 K) as a function of laser power. (c) External photoconductive gain measured in the linear (open square) and nonlinear (solid square) regions of the current−voltage characteristics as a function of laser power. (d) Bias dependence of the photoresponse is shown for various laser powers. Inset: dependence of V_c on P (solid square). Solid line represents a linear fit to the data.

be ~1.3 A/W and G_{ext} = 250% (see Supporting Information, Figure S8 and S9). G_{ext} increases with increasing P both in the linear and nonlinear regions of the $I-V$ characteristics (Figure 3c).

For fixed illumination intensity, the photoresponse initially decreases with increasing bias voltage and after reaching a minimum at bias V_c (which decreases with increasing P), it again increases (Figure 3d and inset). These results suggest that the observed photoconduction cannot be explained by the formation of excitons. Photoexcitons contribute to photoconductivity only when the bound electron hole pairs dissociate to produce free electrons and holes with the aid of either a large electric field[15] or thermal energy,[14] so the photoresponse would become stronger with increasing temperature and/or increasing bias. Our data also excludes the contribution of hot carriers, for which the photoconduction would increase with increasing bias.[27] The samples are placed in high vacuum ($<10^{-6}$ mbar) and the photoresponse is strong at low temperature, so we can safely exclude the photodesorption effect as a cause of the observed photoconduction.[17,18]

In disordered systems like bulk polymers, charge transport generally takes place by phonon assisted hopping from one localized state to another. In these systems, photoconductivity depends on the availability of the long-lived trap states.[1,6] With increasing light intensity, the photoconductive gain decreases due to the saturation of the photoexcited trap states.[28] In our case G_{ext} increases with increasing P both in the linear and nonlinear regions of the $I-V$ characteristics (Figure 3c). Also, for hopping transport the number of charge carriers injected into the sample increases with increasing bias. In the presence of light with energy less than the band gap, photoexcited charge carriers from deeper trap states contribute to the hopping transport. The bias affects the mobility in a density-independent manner,[29] so for fixed illumination intensity the relative contribution of bias to the current enhancement is reduced, and the photoresponse should decrease with increasing bias.

To determine the nature of the photoconduction and to rule out the bolometric effect as a possible mechanism, we have done the following experiments. The nanowires are illuminated by a laser power of 0.9 mW at 4.2 K, and the corresponding threshold voltage is found to be 1.55 V. The same threshold voltage is obtained in the absence of illumination when we increase the temperature to 40 K (Figure 4a). Although the threshold voltages are the same in both cases, the current flowing through the nanowires at 40 K below switching in the absence of illumination (I_{dark} (40 K)) is much larger than that in the presence of 0.9 mW illumination at 4.2 K ($I_{0.9}$ mW(4.2 K)). This result clearly shows that the switching transition is not determined by the amount of current flowing through the sample and also rules out local heating as a cause of the observed photoresponse. The samples are placed in good thermal contact with the coldfinger of the cryostat which also prevents any bolometric contribution.[16] We also did not observe any considerable change in temperature of the nanowires (measured by placing a sensor near the sample) under laser illumination. The time constant for bolometric response is typically 1 to 100 ms,[16] which is shorter than in our system. We have shown earlier that the observed switching transition is not of thermal origin.[24,25] This experiment reconfirms the nonthermal origin of the switching transition. To find out what determines the switching threshold, we measured capacitance near the switching transition by

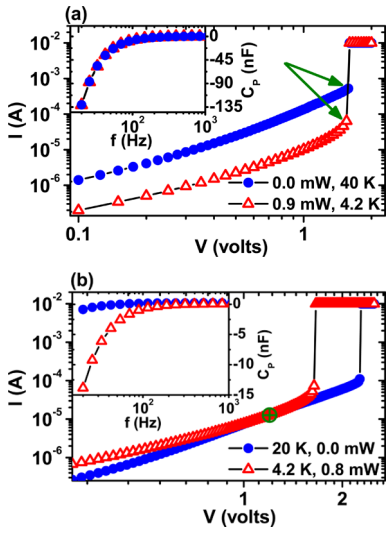

Figure 4. (a) Current–voltage characteristics at 4.2 K in the presence of 0.9 mW illumination (open triangle) and at 40 K in the dark (solid circle). It is clear that though the current flowing through the sample in these two conditions is different, the threshold voltages are the same. Inset: Frequency dependence of the capacitance (measured near the switching transition). (b) Current–voltage characteristics at 20 K in the dark (solid circle) and at 4.2 K in the presence of 0.8 mW illumination (open triangle). Resistance of the sample in these two conditions remains the same over a range of bias near the switching transition. Inset: Frequency dependence of the capacitance, measured (applying 100 millivolt peak-to-peak ac bias superimposed on 1.2 V dc bias) where the dc resistance is the same for these two conditions.

applying 100 millivolt peak-to-peak ac bias superimposed on 1.5 V dc bias. We found that, though the current flowing through the nanowires near the switching transition in the presence of 0.9 mW laser illumination at 4.2 K and in dark at 40 K is markedly different, the measured capacitances are nearly the same (refer to inset of Figure 4a). The capacitance remains negative in the low frequency regime and becomes positive above a certain frequency.[30] We have found that, for the same dc resistance (contribution from the mobile charge carriers) of the sample in two different conditions, (a) at high temperature in absence of illumination and (b) in presence of laser illumination at low temperature, the capacitance is different. Figure 4b shows $I-V$ characteristics measured in the dark at 20 K and in the presence of 0.8 mW laser illumination at 4.2 K; the value of V_{Th} was found to be 2.26 and 1.64 V, respectively. The laser power was chosen in such a way that current flowing through the sample for both cases became the same over a certain range of bias voltage near the switching transition. We have measured capacitance (using 100 millivolt peak-to-peak ac bias superimposed on 1.2 V dc bias) where the dc resistance of the sample in the above two conditions were the same (inset of Figure 4b). We found that the value of measured capacitance is different and the difference increases at low frequency. The magnitude of capacitance is large when V_{Th} is low (1.64 V). We have shown earlier that as the bias voltage approaches toward V_{Th} the negative capacitance state appears and its magnitude increases.[30] The switching transition and observed photoconduction cannot be explained by considering filamentary conduction (see Supporting Information) in these nanowires.

CONCLUSION

These results suggest that free carrier generation, exciton creation, bolometric effect, or Schöttky barrier modulation cannot explain the observed photoresponse. However, it can be explained by photoexcitation of correlated charge carriers present in these nanowires at low temperature.[24,25,30] These correlated carriers remained pinned by the impurities, and above V_{Th} start to slide, showing a switching transition. With increasing carrier concentration (either thermally excited or photogenerated carriers) the pinning potential is screened and V_{Th} decreases. Above a certain temperature (T_m), the correlated state is destroyed (melted) and the switching behavior vanishes. With decreasing pinning strength the melting temperature decreases.[31,32] Our observation of decreasing T_m with increasing P (Figure 2c) is also consistent with this picture. The switching behavior vanishes above 80 K (see Supporting Information, Figure S4) and the photoresponse also becomes vanishingly small above this temperature (Figure 3b left panel), again suggesting that correlated charge carriers are responsible for the observed photoresponse. The bias dependence of the photoresponse (Figure 3d) is also consistent with this picture. However, the initial decrease of the photoresponse up to a certain bias can be accounted for by normal carriers. With increasing bias, the contribution from correlated carriers increases and above V_c it dominates (even before the sliding motion starts) and the photoresponse again increases. With increasing P the relative strength of pinning diminishes, hence correlated carriers start to dominate even at lower bias, thus V_c decreases. The appearance of negative capacitance is also related to the presence of pinned correlated charges in these nanowires.[30] Capacitances of the same magnitude having the same V_{Th} but different current values (inset of Figure 4a) suggest that capacitance magnitude depends on the relative strength of the impurity potential, while the low current for the illuminated sample is due to the low kinetic energy (low temperature) of the carriers. Above the threshold (in the switched state), the photoresponse is very small. This is probably because above V_{Th} the sliding motion starts, so the screening of the impurity potential by photogenerated carriers does not have any further considerable effect on the motion of the correlated charge carriers. In conclusion, we have shown novel photoresponse properties of polymer nanowires

which are absent in the bulk polymer. The origin of the observed photoresponse is not bolometric or excitonic, nor can be it explained by free carrier generation or Schöttky barrier modulation. However, it is consistent with the photoexcitation of correlated charge carriers whose emergence in organic nanostructures is of prime interest.

METHODS

Nanowire Synthesis. Polypyrrole nanowires of various diameters were fabricated by a template−based synthesis technique by a chemical route, taking Pyrrole as a monomer and ferric chloride ($FeCl_3$) as oxidizing agent in a 1:5 ratio. All the samples were prepared using 0.1 M HCl solution, and prior to the synthesis the Pyrrole monomer was vacuum distilled. The polycarbonate membranes of various pore diameters (50, 100, 200, and 400 nm) were placed between the compartments of a two-compartment glass cell; the monomer is added in one cell and oxidizing agent ($FeCl_3$) into another cell. The polymerization reaction takes place inside each pore, and polypyrrole nucleates at the pore wall forming a tube. With increasing polymerization time, the tube wall thickness increases and finally the pores get completely filled up to form nanowires.

Photoconduction Measurements. For photoconduction measurements, we deposited 10 nm thick and 2 mm diameter circular gold pads on both sides of the membrane containing nanowires (see Figure 1b). More than 95% of the laser light, of 632.8 nm wavelength, can penetrate through this gold layer. The samples were illuminated by a He−Ne laser (Spectra Physics, model 117A), having a maximum output power of 4.5 mW at 632.8 nm. The intensity was measured using a calibrated photodetector (Newport, model 818-SL) with the help of a dual channel power meter (Newport, model 2832-C). Voltage biased measurements were carried out in a two-probe configuration using a Keithley 2400 source-measure unit (current compliance set to 10 mA). Current biased measurements were done by driving current using the Keithley 2400 source meter, and the voltage is measured using an Agilent 34420A nanovoltmeter. Low temperature measurements were done in a Janis closed cycle refrigerator operated between 4 and 300 K, and the samples were illuminated through its optical window (see Figure 1c). Before measurements, actual laser intensity at the sample position was measured, and it was found that nearly 94% laser light penetrates through the window (see Supporting Information, Figure S12). Sample temperature was controlled using a 50 Ohm heater installed near the sample holder and a LakeShore 340 temperature controller and a Si-diode sensor. During the measurements, the sample space was kept in $<10^{-6}$ mbar vacuum.

Conflict of Interest: The authors declare no competing financial interest.

Supporting Information Available: Figures S1 to S12; ruling out filamentary conduction. This material is available free of charge via the Internet at http://pubs.acs.org.

Acknowledgment. The authors would like to thank Janice Wynn Guikema and Abhisakh Sarma for their help.

REFERENCES AND NOTES

1. Konstantatos, G.; Howard, I.; Fischer, A.; Hoogland, S.; Clifford, J.; Klem, E.; Levina, L.; Sargent, E. H. Ultrasensitive Solution-Cast Quantum Dot Photodetectors. *Nature* **2006**, *442*, 180–183.
2. Konstantatos, G.; Sargent, E. H. Nanostructured Materials for Photon Detection. *Nat. Nanotechnol.* **2010**, *5*, 391–400.
3. McDonald, S. A.; Cyr, P. W.; Levina, L.; Sargent, E. H. Photoconductivity from PbS-Nanocrystal/Semiconducting Polymer Composites for Solution-Processible, Quantum-Size Tunable Infrared Photodetectors. *Appl. Phys. Lett.* **2004**, *85*, 2089–2091.
4. Sargent, E. H. Solar Cells, Photodetectors, and Optical Sources from Infrared Colloidal Quantum Dots. *Adv. Mater.* **2008**, *20*, 3958–3964.
5. Gabor, N. M.; Zhong, Z.; Bosnick, K.; Park, J.; McEuen, P. L. Extremely Efficient Multiple Electron−Hole Pair Generation in Carbon Nanotube Photodiodes. *Science* **2009**, *325*, 1367–1371.
6. Sofos, M.; Goldberger, J.; Stone, D. A.; Allen, J. E.; Ma, Q.; Herman, D. J.; Tsai, W. W.; Lauhon, L. J.; Stupp, S. I. A Synergistic Assembly of Nanoscale Lamellar Photoconductor Hybrids. *Nat. Mater.* **2009**, *8*, 68–75.
7. Gratzel, M. Photovoltaic and Photoelectrochemical Conversion of Solar Energy. *Phil. Trans. R. Soc. A* **2007**, *365*, 993–1005.
8. Huynh, W. U.; Dittmer, J. J.; Alivisatos, A. P. Hybrid Nanorod-Polymer Solar Cells. *Science* **2002**, *295*, 2425–2427.
9. Scharber, M. C.; Mühlbacher, D.; Koppe, M.; Denk, P.; Waldauf, C.; Heeger, A. J.; Brabec, C. J. Design Rules for Donors in Bulk Heterojunction Solar Cells—Towards 10% Energy-Conversion Efficiency. *Adv. Mater.* **2006**, *18*, 789–794.
10. Peumans, P.; Yakimov, A.; Forrest, S. R. Small Molecular Weight Organic Thin-Film Photodetectors and Solar Cells. *J. Appl. Phys.* **2003**, *93*, 3693–3723.
11. Liu, Y.; Wang, H.; Dong, H.; Tan, J.; Hu, W.; Zhan, X. Synthesis of a Conjugated Polymer with Broad Absorption and Its Application in High-Performance Phototransistors. *Macromolecules* **2012**, *45*, 1296–1302.
12. Liu, Y.; Wang, H.; Dong, H.; Jiang, L.; Hu, W.; Zhan, X. High Performance Photoswitches Based on Flexible and Amorphous D−A Polymer Nanowires. *Small* **2013**, *9*, 294–299.
13. Liu, Y.; Dong, H.; Jiang, S.; Zhao, G.; Shi, Q.; Tan, J.; Jiang, L.; Hu, W.; Zhan, X. High Performance Nanocrystals of a Donor−Acceptor Conjugated Polymer. *Chem. Mater.* **2013**, *25*, 2649–2655.
14. Matsuoka, Y.; Fujiwara, A.; Ogawa, N.; Miyano, K.; Kataura, H.; Maniwa, Y.; Suzuki, S.; Achiba, Y. Temperature Dependence of Photoconductivity at 0.7 eV in Single-Wall Carbon Nanotube Films. *Sci. Technol. Adv. Mater.* **2003**, *4*, 47–50.
15. Wang, F.; Dukovic, G.; Brus, L. E.; Heinz, T. The Optical Resonances in Carbon Nanotubes Arise from Excitons. *Science* **2005**, *308*, 838–841.
16. Itkis, M. E.; Borondics, F.; Yu, A.; Haddon, R. C. Bolometric Infrared Photoresponse of Suspended Single-Walled Carbon Nanotube Films. *Science* **2006**, *312*, 413–416.
17. Katz, O.; Garber, V.; Meyler, B.; Bahir, G.; Salzman, J. Gain Mechanism in GaN Schöttky Ultraviolet Detectors. *Appl. Phys. Lett.* **2001**, *79*, 1417–1419.
18. Soci, C.; Zhang, A.; Xiang, B.; Dayeh, S. A.; Aplin, D. P. R.; Park, J.; Bao, X. Y.; Lo, Y. H.; Wang, D. ZnO Nanowire UV Photodetectors with High Internal Gain. *Nano Lett.* **2007**, *7*, 1003–1009.
19. Hu, Y.; Zhou, J.; Yeh, P.-H.; Li, Z.; Wei, T.-Y.; Wang, Z. L. Supersensitive, Fast-Response Nanowire Sensors by Using Schöttky Contacts. *Adv. Mater.* **2010**, *22*, 3327–3332.

20. Kersting, R.; Lemmer, U.; Deussen, M.; Bakker, H. J.; Mahrt, R. F.; Kurz, H.; Arkhipov, V. I.; Bässler, H.; Göbe, E. O. Ultrafast Field-Induced Dissociation of Excitons in Conjugated Polymers. *Phys. Rev. Lett.* **1994**, *73*, 1440–1443.
21. Barth, S.; Bässler, H. Intrinsic Photoconduction in PPV-Type Conjugated Polymers. *Phys. Rev. Lett.* **1997**, *79*, 4445–4448.
22. Moses, D.; Wang, J.; Yu, G.; Heeger, A. J. Temperature-Independent Photoconductivity in Thin Films of Semiconducting Polymers: Photocarrier Sweep-out Prior to Deep Trapping. *Phys. Rev. Lett.* **1998**, *80*, 2685–2688.
23. Mihailetchi, V. D.; Koster, L. J. A.; Hummelen, J. C.; Blom, P. W. M. Photocurrent Generation in Polymer Fullerene Bulk Heterojunctions. *Phys. Rev. Lett.* **2004**, *93*, 216601.
24. Rahman, A.; Sanyal, M. K. Observation of Charge Density Wave Characteristics in Conducting Polymer Nanowires: Possibility of Wigner Crystallization. *Phys. Rev. B* **2007**, *76*, 045110.
25. Rahman, A.; Sanyal, M. K. Novel Switching Transition of Resistance Observed in Conducting Polymer Nanowires. *Adv. Mater.* **2007**, *19*, 3956–3960.
26. Yakushi, K.; Lauchlan, L. J.; Clarke, T. C.; Street, G. B. Optical Study of Polypyrrole Perchlorate. *J. Chem. Phys.* **1983**, *79*, 4774–4778.
27. Mohite, A.; Chakraborty, S.; Gopinath, P.; Sumanasekera, G. U.; Alphenaar, B. W. Displacement Current Detection of Photoconduction in Carbon Nanotubes. *Appl. Phys. Lett.* **2005**, *86*, 061114.
28. Muñoz, E.; Monroy, E.; Garrido, J. A.; Izpura, I.; Sánchez, F. J.; Sánchez-García, M. A.; Calleja, E.; Beaumont, B.; Gibart, P. Photoconductor Gain Mechanisms in GaN Ultraviolet Detectors. *Appl. Phys. Lett.* **1997**, *71*, 870–872.
29. Pasveer, W. F.; Cottaar, J.; Tanase, C.; Coehoorn, R.; Bobbert, P. A.; Blom, P. W. M.; de Leeuw, D. M.; Michels, M. A. J. Unified Description of Charge Carrier Mobilities in Disordered Semiconducting Polymers. *Phys. Rev. Lett.* **2005**, *94*, 206601.
30. Rahman, A.; Sanyal, M. K. Negative Capacitance in Wigner Crystal Forming Polymer Nanowires. *Appl. Phys. Lett.* **2009**, *94*, 242102.
31. Tsukada, M. Two-Dimensional Crystallization of the Electrons in MOS Structures Induced by Strong Magnetic Field. *J. Phys. Soc. Jpn.* **1977**, *42*, 391–398.
32. Chen, Y. P.; Sambandamurthy, G.; Wang, Z. H.; Lewis, R. M.; Engel, L. W.; Tsui, D. C.; Ye, P. D.; Pfeiffer, L. N.; West, K. W. Melting of a 2D Quantum Electron Solid in High Magnetic Field. *Nat. Phys.* **2006**, *2*, 452–455.